Synthetic Aperture Radar Remote Sensing and Damage Detection

Masashi Matsuoka
Tokyo Institute of Technology

Interpretation Example (Optics)
– earthquake damage -

- Damaged areas may be inaccessible to imaging because of clouds and cloud shadows.

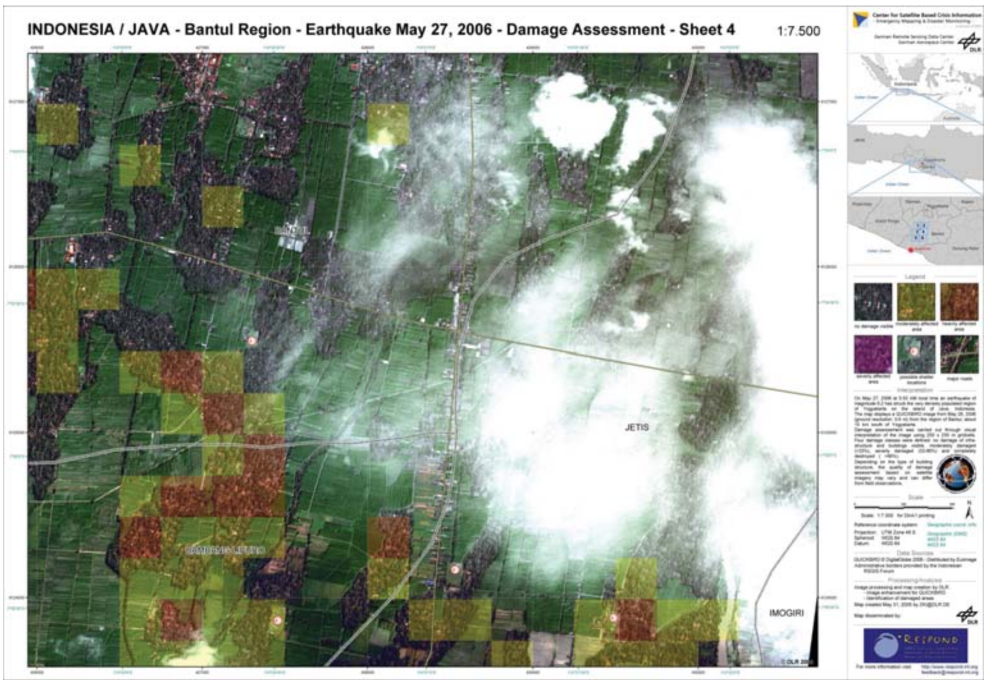

Source: DLR

Satellite Images Observed by Microwave and Optical Sensors

Microwave sensors receive microwaves, which is longer wavelength than visible light and infrared rays, and observation is not affected by day, night or weather.
The active sensor aboard earth observation satellite emits microwaves and observes microwaves reflected by land surface.

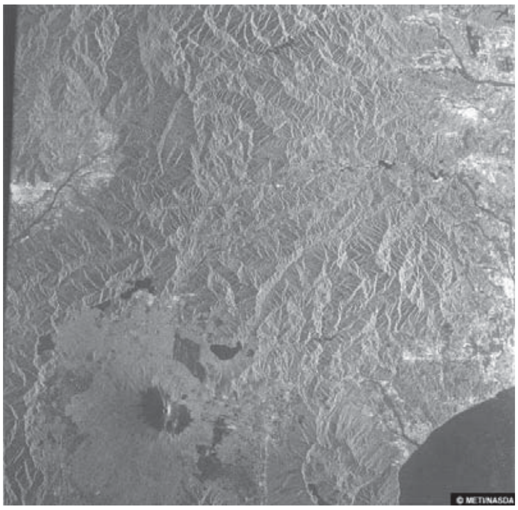

JERS-1/SAR

LANDSAT-5/TM

Radar (Radio Detection And Ranging)

- **A radar system has three primary functions:**
  - It transmits microwave (radio) signals towards a scene
  - It receives the portion of the transmitted energy backscattered from the scene
  - It observes the strength (detection) and the time delay (ranging) of the return signals.
- **Therefore, measurement of**
  - Time delay
  - Power
  - Phase

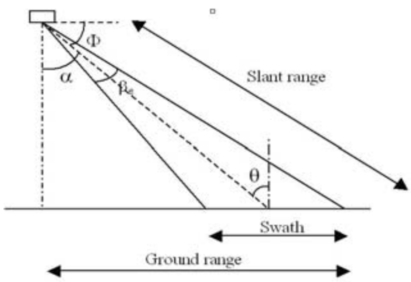

Operating Principle of Side-Looking Rader

Microwave transmitting and receiving

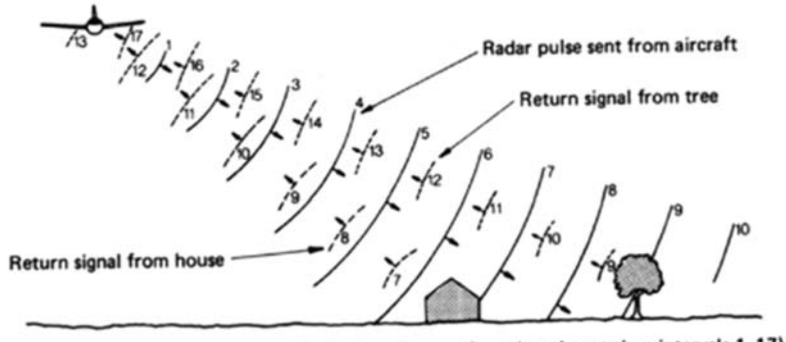

(a) Propagation of one radar pulse (indicating the wavefront location at time intervals 1-17)

Signal

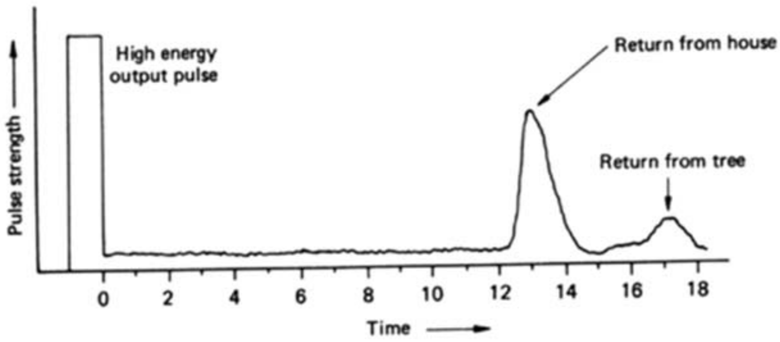

(b) Resulting antenna return

Contents of SAR Data

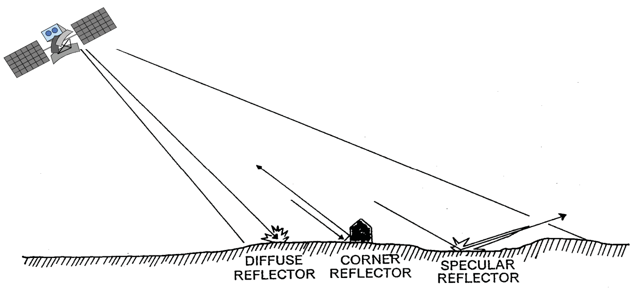

Amplitude (Intensity) Image
Backscattering Coefficient [dB]

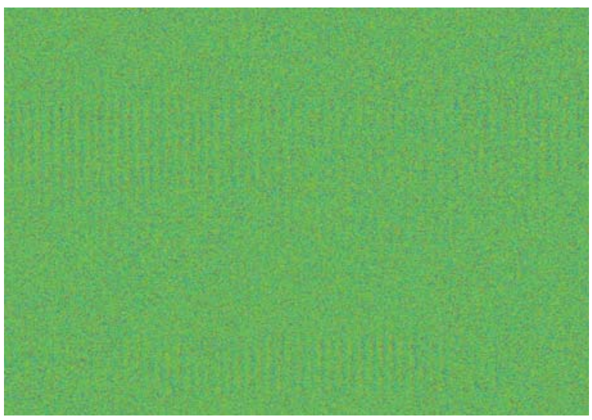

Phase Image
-π ~ π [rad]

ERS image taken on 1995/5/23

D-InSAR Application – Coseismic displacement

The 1995 Kobe earthquake

1992/9~1995/2

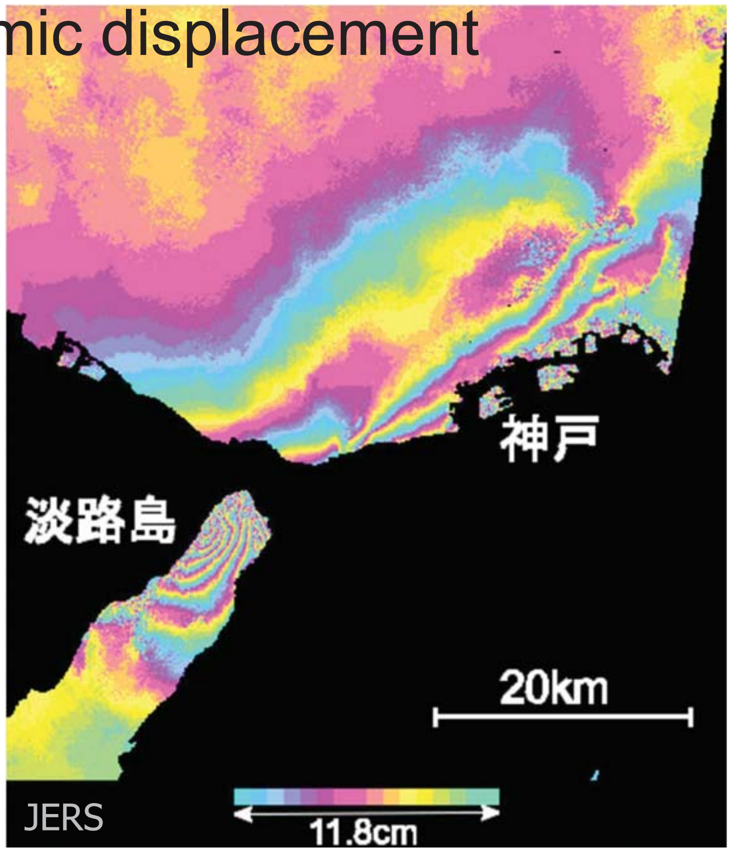

Source: GSI

Visual Damage Interpretation?

Before the Kobe earthquake

After the Kobe earthquake

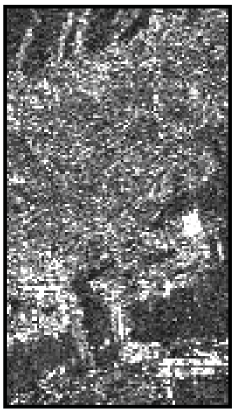

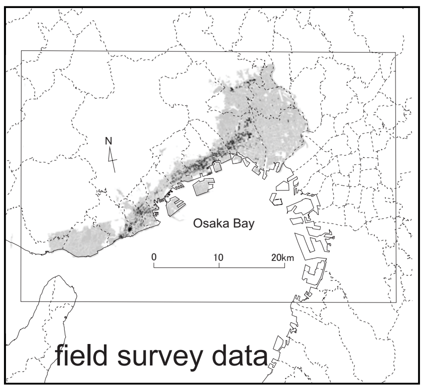

field survey data

- It is difficult to interpret damaged areas due to earthquakes visually.
- To use SAR images effectively for damage detection, appropriate image-processing is essential.

Microwave Scattering in the Areas of Building Damage

- Backscattering coefficient (intensity)

  buildings > damaged area or open space

- Difference in intensity (after – before)

  damage < no damage

- Correlation of intensity

  damage < no damage

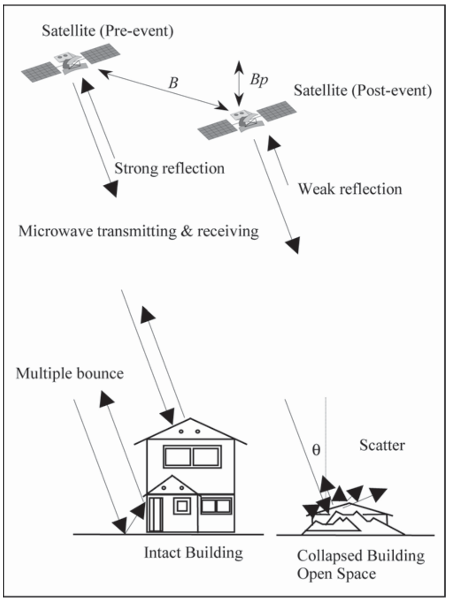

Schematic diagram for detecting building damage using repeat-pass radar observation

Difference in Backscattering Coefficient and Correlation

Difference:

$$d = 10 \cdot \log_{10} \bar{I}a_i - 10 \cdot \log_{10} \bar{I}b_i$$

Correlation:

local window size is optional

$$r = \frac{N\sum_{i=1}^{N} Ia_i Ib_i - \sum_{i=1}^{N} Ia_i \sum_{i=1}^{N} Ib_i}{\sqrt{\left(N\sum_{i=1}^{N} Ia_i^2 - \left(\sum_{i=1}^{N} Ia_i\right)^2\right) \cdot \left(N\sum_{i=1}^{N} Ib_i^2 - \left(\sum_{i=1}^{N} Ib_i\right)^2\right)}}$$

where i is the sample number, and Ia_i and Ib_i are the digital numbers of the post- and pre-images, respectively. $\bar{I}a_i$ and $\bar{I}b_i$ are the corresponding averaged digital numbers over the surroundings of pixel i within a (13 × 13) pixel window; the total number of pixels N within this window is (169), which is used to compute the two indices.

Images before and after the January 17, 1995 Kobe Earthquake

ERS image taken on 1994/10/12

ERS image taken on 1995/5/23

- Intensity image matching
  - Backscattering coefficient (Sigma-nought) was converted from multi-look amplitude (power) value.

GIS-based Damage Survey Data of the 1995 Kobe Earthquake

- The building damage data based on detailed survey results, digitized by the Building Research Institute.
- The areas of boiled sand deposits were survey by Hamada et al.

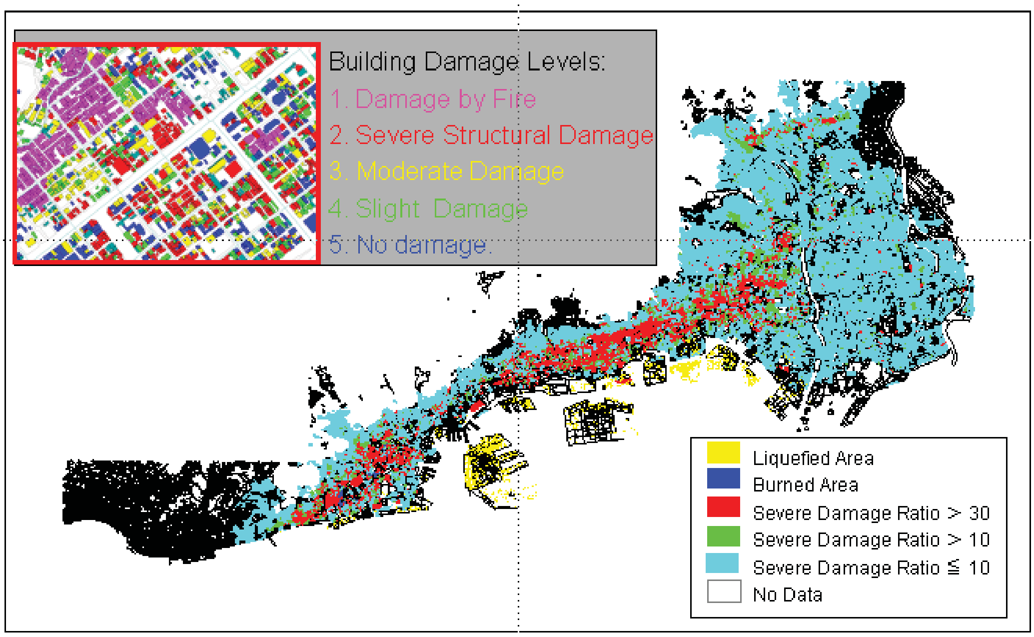

Final Damage Report of the 1995 Hyogo-ken Nanbu Earthquake; Building Research Institute: Tsukuba, Japan, 1996; p. 303

Difference and Correlation Images

- Difference in intensity
  - Difference in backscattering coefficient was calculated between pre- and post-event Lee filtered SAR intensity images by averaging a 13 x 13 window.
- Correlation of intensity
  - Correlation coefficient for two acquisition data was calculated within a same window using amplitude (power) value.

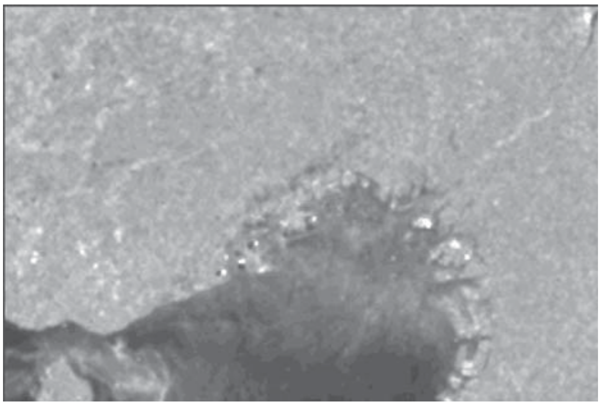

Difference (after – before)

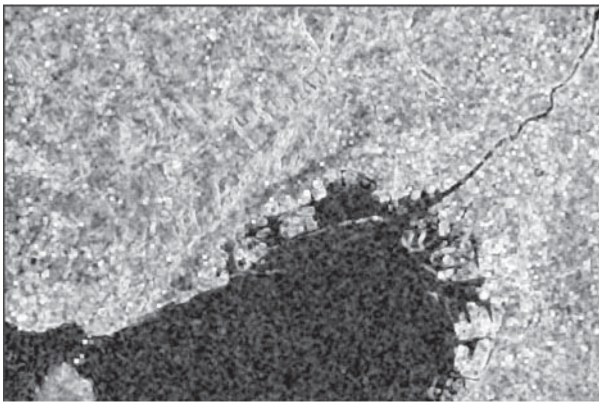

Correlation

Proposed Discriminant Score *z*

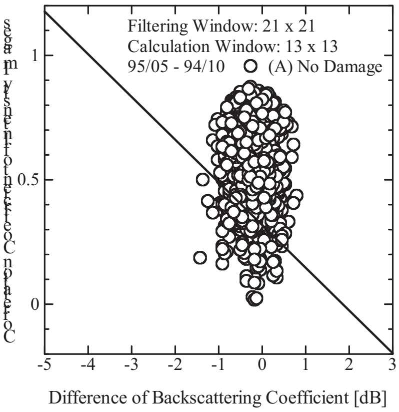

Pixels for no damage

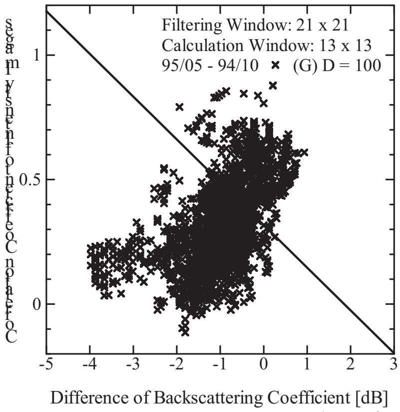

Pixels for catastrophic damaged (severe damage ratio = 100%)

$$z = -2.140\, d - 12.465\, r + 4.183$$

d : difference in backscattering coefficient (dB) (after – before)

r : correlation coefficient

Flow of Damage Detection

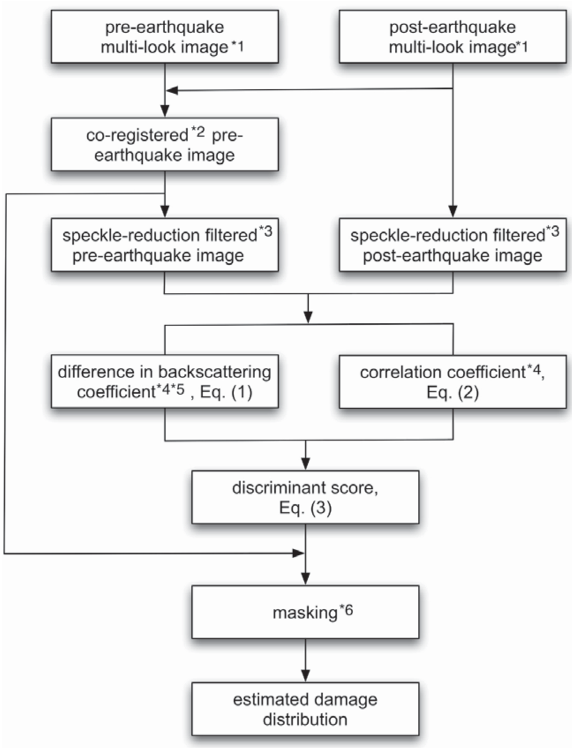

$$z = -2.140\,d - 12.465\,r + 4.183 \qquad (3)$$

d : difference in backscattering coefficient (dB) (after – before)

r : correlation coefficient

Note:

*1 Pixel size: Equal to the size of spatial resolution of satellite's sensor
Digital number: Power of radar brightness

*2 Tie point selection: Template matching
Registration: Affine transformation
Resampling: Nearest-Neighbor method

*3 Filter type: Lee filter
Window size: 21 x 21 pixel

*4 Window size: 13 x 13 pixel

*5 Difference (post - pre): Average value within a window

*6 Threshold value: -5dB

Result and Comparison with Ground Truth Data

Illumination direction of radar

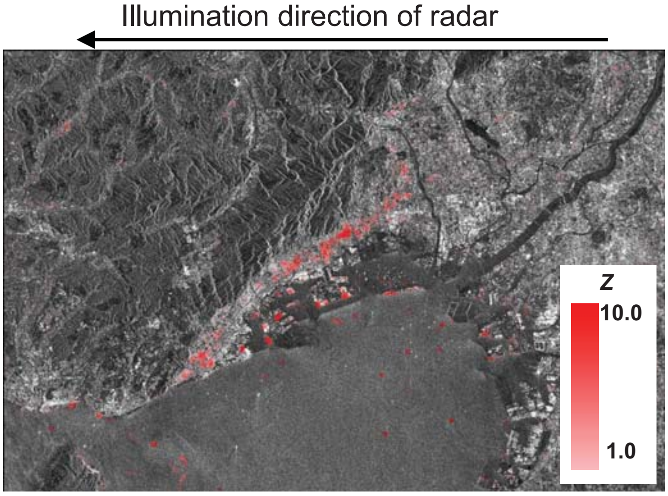

- ERS
  (1994/6/3 – 1995/5/23)

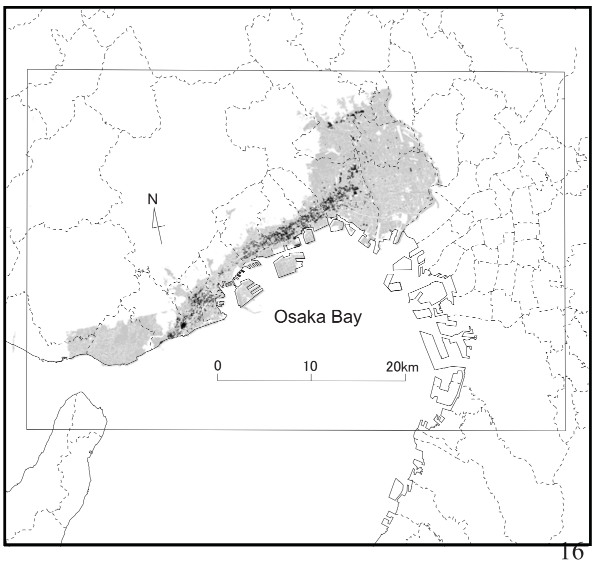

- Ground Truth Data
  (BRI, 1996)
- Black:
  Severe damage ratio > 30%

Final Damage Report of the 1995 Hyogo-ken Nanbu Earthquake; Building Research Institute: Tsukuba, Japan, 1996; [CD-ROM], p. 303 (in Japanese).

September 12, 1993 Hokkaido Nansei-oki, Japan Earthquake

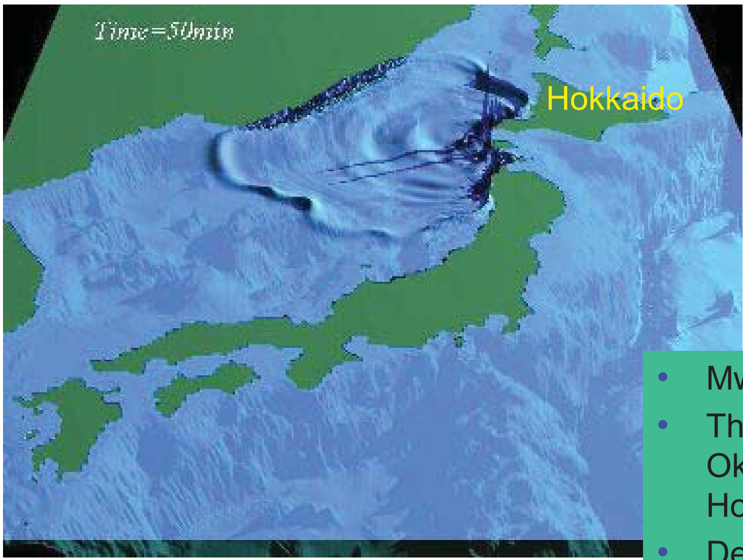

© Y. Okamoto, Osaka Kyoiku Univ.

- Mw = 7.7
- The epicenter was located near Okushiri Island, south-western Hokkaido. Focal depth of 34 km
- Death toll about 230
- Tsunami and fires destroyed many houses. 1,157 houses collapsed or heavily damaged

Result from JERS/SAR Images Before and After the Earthq.

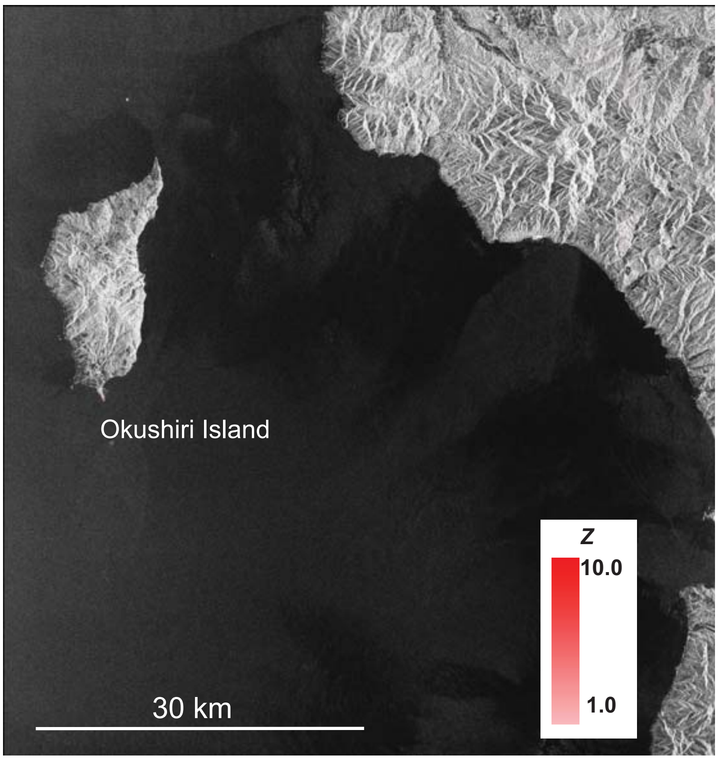

- JERS 40 days after EQ (1993/7/8 – 1993/8/21)

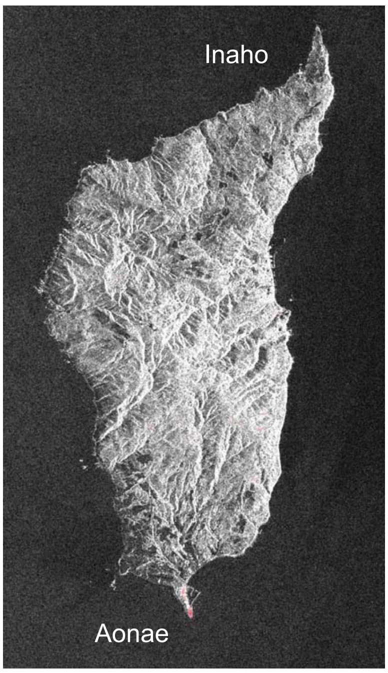

©METI and JAXA

Result and Comparison with Aerial Photos (Aonae)

Post-event (1993/7/18)

Pre- and Post-events (1993/7/8 -1993/8/21)

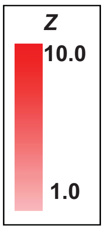

Pre-event (1990/10/29)

Pre-events pair (1993/5/25-1993/7/8)

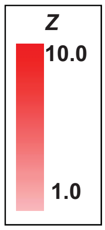

Result from ERS/SAR Images Before and After the Earthq.

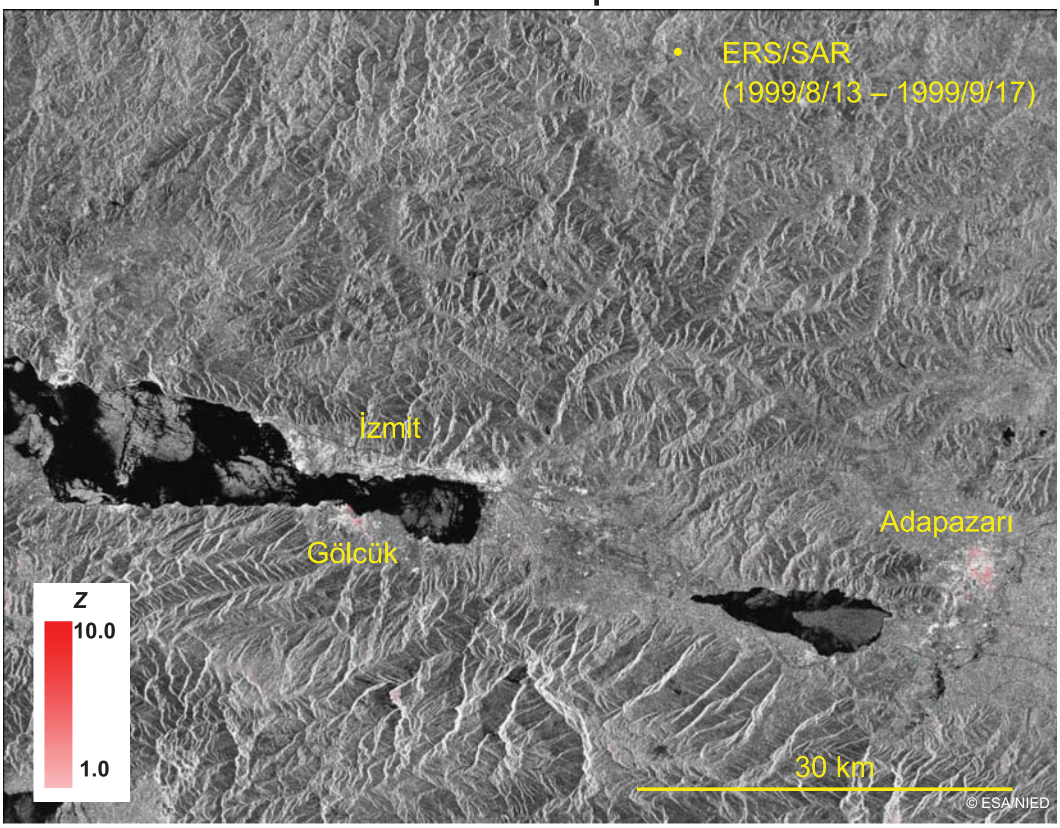

Field Survey Result

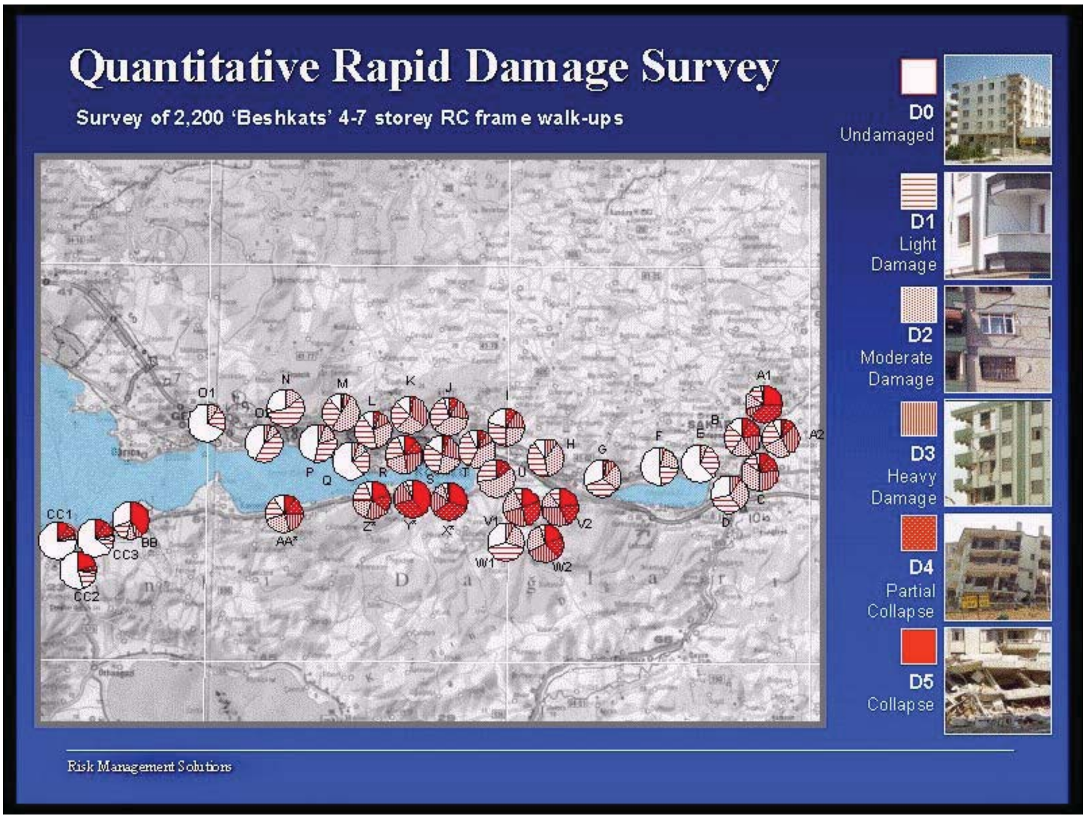

Change Detection Technique for Slope Failure

- The previous damage detection technique is mainly based on the phenomenon of decreasing cardinal effect in high-densely built-up areas after an earthquake using only two scenes taken before and after the earthquake.
- For the areas except for urban, another damage detection technique is needed.
- Evaluation and comparison with temporal changes using a greater number of scenes is possible solution.
- Damaged areas might show grater change than temporal one.
- The temporal change is estimated from a pre-event.

Slope Failure Damage Distribution

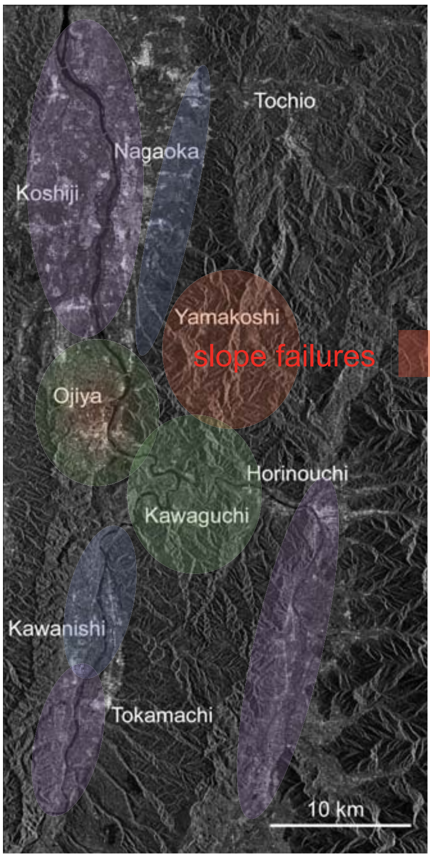

Schematic distribution of damages

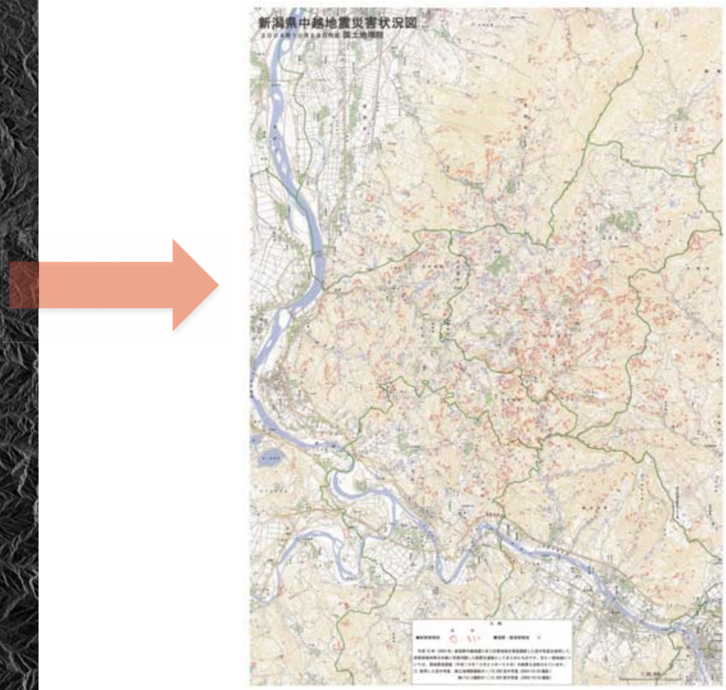

Visual damage interpretation of slope failure by Geographical Survey Institute

Change Detection Method (for Slope Failure)

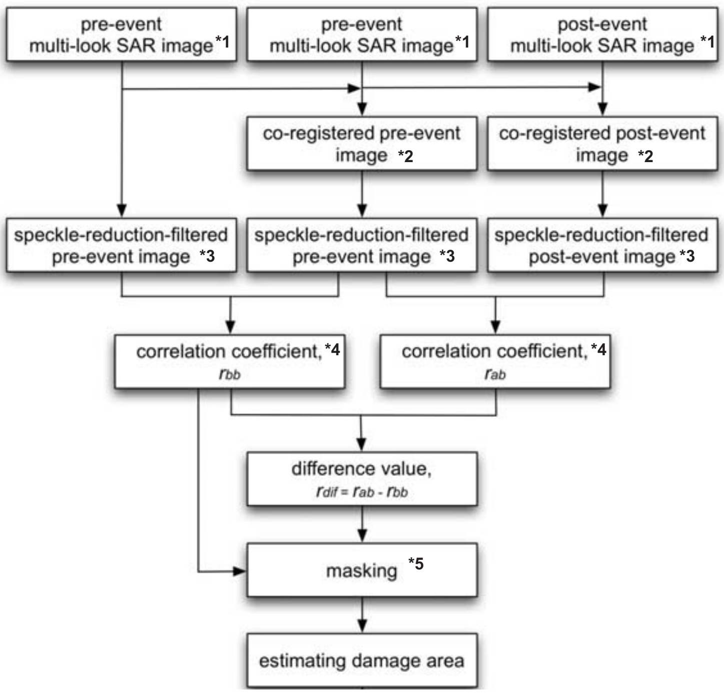

The crux of this technique for estimating building damage involves calculating the difference between the correlation coefficients of pre-seismic and co-seismic pairs to minimize the effect of surficial changes over time.

Note:

*1 Pixel size: Equal to the size of spatial resolution of satellite's sensor
Pixel value: Power

*2 Tie point selection: Correlation method
Registration: Affine transformation
Resampling: Nearest-Neighbor method

*3 Filter type: Lee filter
Window size: 21 x 21 pixel

*4 Window size: 13 x 13 pixel

*5 Threshold value: $r_{bb} < 0.8$

Distribution of Difference in Correlation Coefficient

Areas selected by correlation coefficient, from a pair of pre-event images, which is more than 0.8.

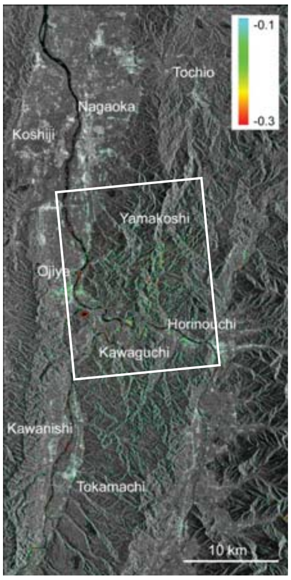

Yamakoshi village (slope failures)

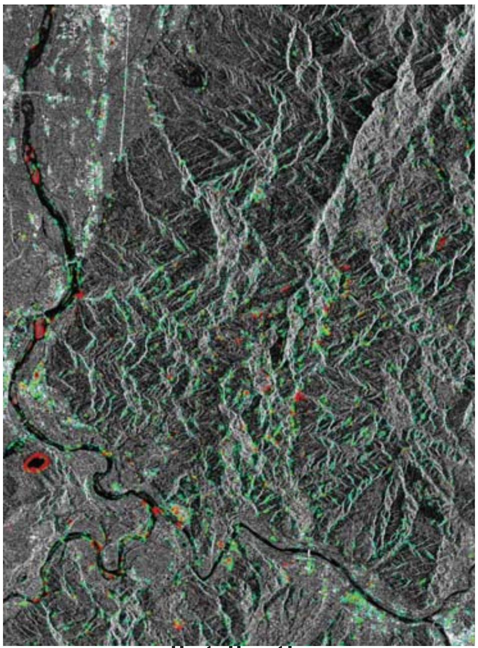

r_{dif} distribution

Slope-failures

By Geographical Survey Institute

2005.10.8 Northern Pakistan Earthquake

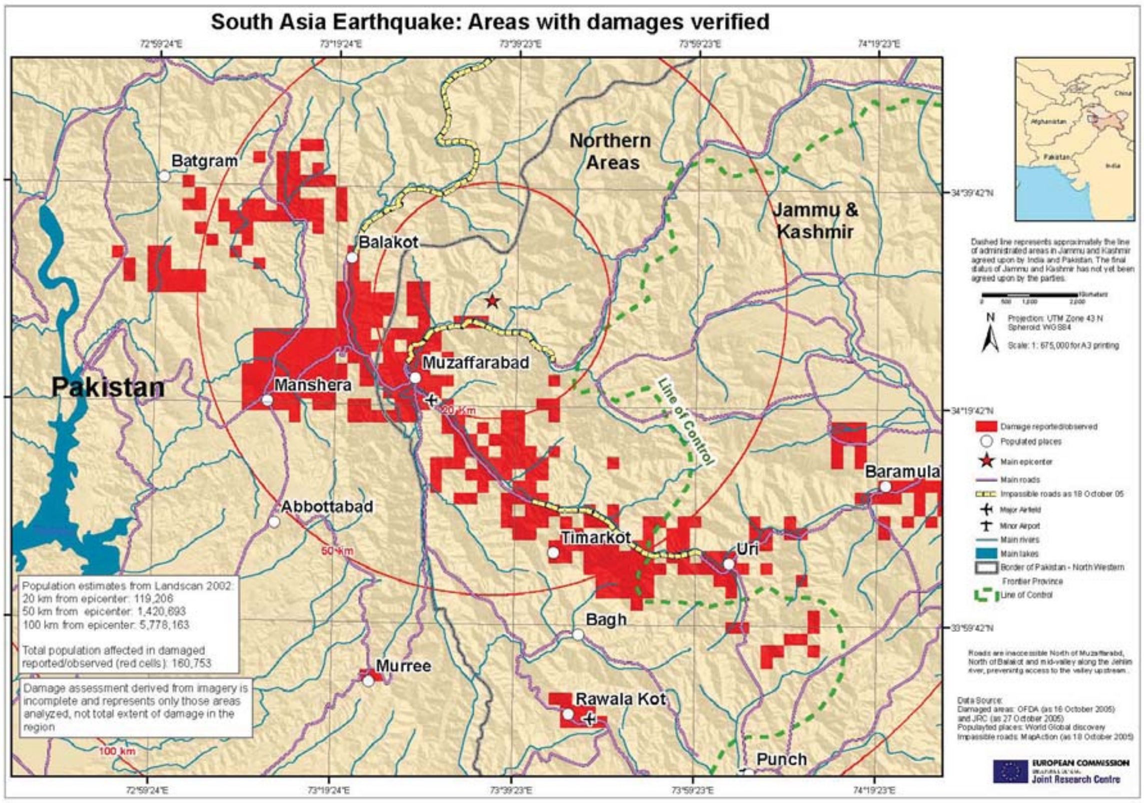

European Commission Joint Res. Ctr.